Effect of Holding Time in the (α + γ) Temperature Range on Toughness of Specially Austempered Ductile Iron

TOSHIRO KOBAYASHI and SHINYA YAMADA

Austempered ductile iron (ADI) finds wide application in the industry because of its high strength and toughness. The QB' process has been developed to produce a fine microstructure with high fracture toughness in ADI. This process involves reaustenitizing a prequenched ductile iron in the (α + γ) temperature range followed by an isothermal treatment in the bainitic transformation temperature range. In the present work, the effect of holding time in the (α + γ) temperature range on the structure and un-notched toughness of ADI has been studied. Prior to the austempering treatment, the as-cast ductile iron was heat treated to obtain martensitic, ferritic, and pearlitic matrix structures. In the case of prequenched material (martensitic matrix), the un-notched impact toughness increased as a function of holding time in the (α + γ) temperature range. The reaustenitization heat treatment also resulted in the precipitation of fine carbide particles, identified as $(Fe,Cr,Mn)_3C$. It was shown that the increase in holding time in the (α + γ) temperature range leads to a reduction in the number of carbide particles. In the case of a ferritic prior structure, a long duration hold in the (α + γ) temperature range resulted in the coarsening of the structure with a marginal increase in the toughness. In the case of a pearlitic prior structure, the toughness increased with holding time. This was attributed to the decomposition of the relatively stable carbide around the eutectic cell boundary with longer holding times.

I. INTRODUCTION

AUSTEMPERED ductile iron (ADI) is currently used widely in the place of cast steel and weld components because of its high strength, wear resistance, and toughness. The austempering cycle involves soaking the ductile iron above the upper critical temperature (austenitization), followed by a quench fast enough to prevent the transformation of austenite to pearlite and an isothermal hold in the bainitic transformation temperature range to transform the austenite to ferrite and stable high-carbon retained austenite. In general, however, unstable retained austenite, called the γ pool, persists around the eutectic cell boundary. The γ pool, an unreacted constituent not stabilized by the concentration of carbon, degrades the toughness and machinability of ADI.[1,2] This has been one of the problems in putting ADI to practical use.

The authors had previously reported the QB' process as a method to further toughen the ADI with least sacrifice in the strength level.[3] This process consists of prequenching (Q process) the ductile iron followed by reaustenitizing in the (α + γ) temperature range* and an isothermal treatment (B' process) in the bainitic transformation temperature range. Toughened ADI, produced by the QB' process, shows high fracture toughness compared with the ordinary ADI. The QB' process provides a fine ausferritic microstructure and stable retained austenite around both the graphite/matrix interface and the eutectic cell boundary, which are the crack initiation sites in the ductile iron. The martensitic microstructure introduced by prequenching has a large number of precipitation sites for the acicular ferrite to form, and thus, a uniform ausferritic microstructure without the γ pool is obtained. Moreover, the stability of retained austenite in the final microstructure is increased due to the fact that the alloying elements concentrate in the austenite phase during holding in the (α + γ) temperature range.

It is generally recognized that the structure and mechanical properties of the toughened ADI are determined by the composition, heat treatment conditions, and microstructure of ductile iron before austempering. The favorable impact of microsegregation of an alloying element like Ni or Cu and the advantages of effecting preferential austenitization in the matrix by heating in the (α + γ) temperature range have been covered in previous articles.[3–7] The toughness of ADI produced by the QB' process increased following longer holding times in the (α + γ) temperature range.[6,7] In order to optimize the heat treatment conditions, for producing the toughened ADI, an improved understanding is

*The austenitizing temperature range indicated here corresponds to the (α + γ + graphite) region. In this article, this is indicated in short hand as the (α + γ) temperature range.

TOSHIRO KOBAYASHI, Professor, is with the Department of Production Systems Engineering, Toyohashi University of Technology, Toyohashi 441, Japan. SHINYA YAMADA, Dr. Eng., formerly Graduate Student, Department of Production Systems Engineering, Toyohashi University of Technology, is with the RRD Center, AISIN TAKAOKA Co., Ltd., Toyota 473, Japan.

Manuscript submitted March 10, 1995.

Table I. Chemical Composition of Test Material (Mass Pct)

C	Si	Mn	P	S	Mg	Ni	Cr
3.30	1.99	0.67	0.029	0.012	0.049	2.30	0.16

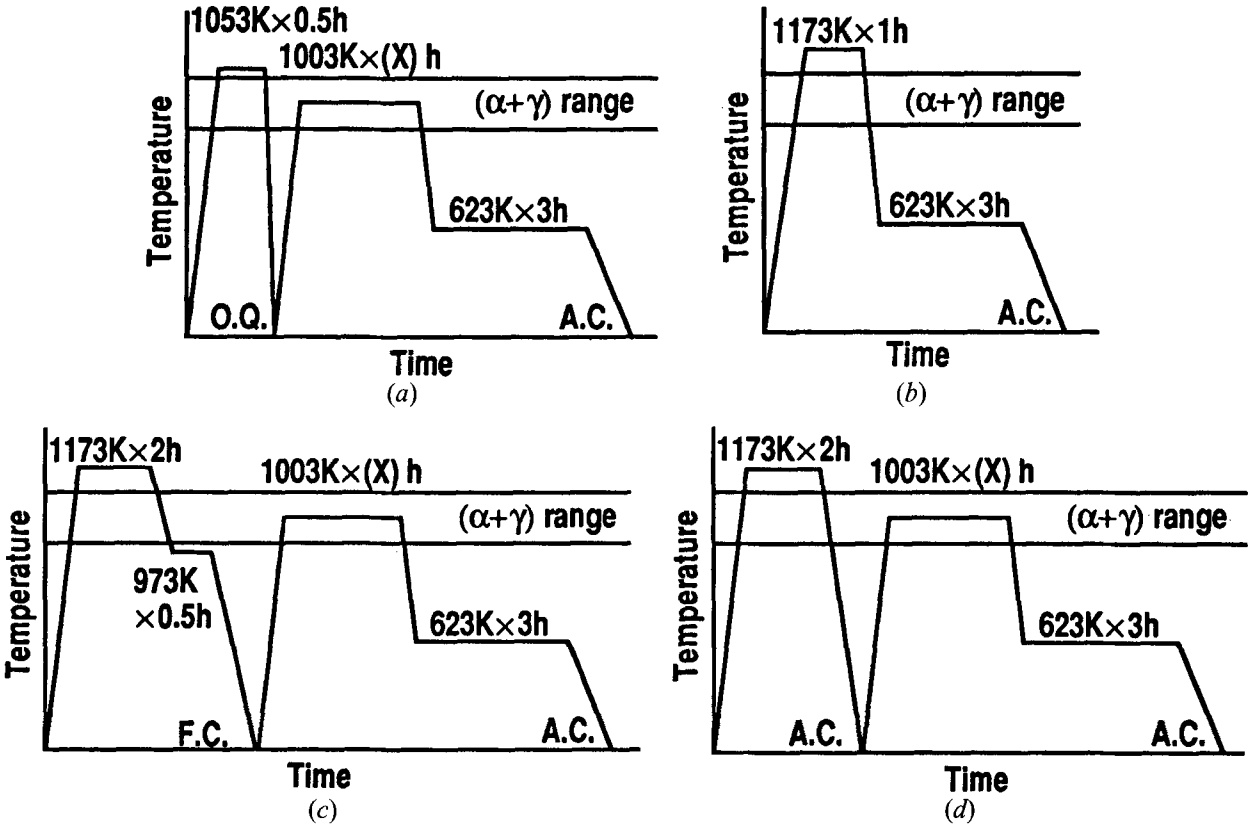

Fig. 1—Heat treatment processes: (*a*) QB' process, (*b*) ordinary austempering, (*c*) FB' process, and (*d*) PB' process.

needed with respect to the changes occurring in the microstructure, the extent of toughness variation, and the effect of prior structure. This article addresses the toughness and microstructural aspects of ADI, with prior martensitic, ferritic, and pearlitic structures, as a function of holding time in the (α + γ) temperature range.

II. EXPERIMENTAL PROCEDURE

A. *Material, Heat Treatment, and Test Specimen*

The material, cast in Y block with a thickness of 35 mm, had an almost fully pearlitic matrix in the as-cast condition. Table 1 shows the chemical composition of the material. The alloying addition of 2.3 pct Ni was chosen based on earlier experience.[7] The nickel addition was made with an intent to effect favorable microsegration around the graphite nodules, so that preferential austenitization would take place in these regions when the material was subjected to heating in the (α + γ) temperature range.

Figure 1(a) shows the QB' process featuring the austenitization at 780 °C for 0.5 hours, water quenching (Q process), reaustenitization at 730 °C in the (α + γ) temperature range for 0.5, 1, 3, 7, 15, and 50 hours, and isothermal treatment at 350 °C for 3 hours (B' process). Figure 1(b) shows the conventional austempering process consisting of austenitization at 900 °C for 1 hour and isothermal treatment at 350 °C for 3 hours. The treated iron has a strength of 1000 MPa with elongation of 8 pct. Furthermore, in the present work, the ferritic (F) and pearlitic (P) ductile irons were also subjected to the B' process. The ferritic and pearlitic structures were obtained in the ductile iron through heat treatment. Figures 1(c) and (d) show, respectively, the details of heat treatment with respect to the FB' and PB' processes.

Half-size un-notched Charpy-type specimens (5 × 10 × 55 mm) were used for the impact tests. The specimens were machined from the middle of the heat-treated Y-block sections.

B. *Instrumented Charpy Impact Test*

In order to examine the effect of heat treatment on the toughness properties, instrumented Charpy impact tests were performed in the temperature range −196 °C to 20 °C. A computer aided instrumented Charpy impact testing system (CAI system),[8,9] of 490 J capacity, developed by one of the authors, was used to obtain the load *vs* load-point displacement curve and the absorbed energy. In the CAI system, the load is measured by a semiconductor strain gage attached to the hammer edge portion, and the load-point displacement is measured by a film-potentiometer located on the rotating axis of the hammer.

The initial loading velocity was 3 m/s in all the tests. Subsequent to the impact test, lateral expansion measurements (on the broken halves) were made and the values were expressed as a percentage of the initial thickness.

Vickers hardness was measured in the center of the heat-treated material, with a load of 10 kg.

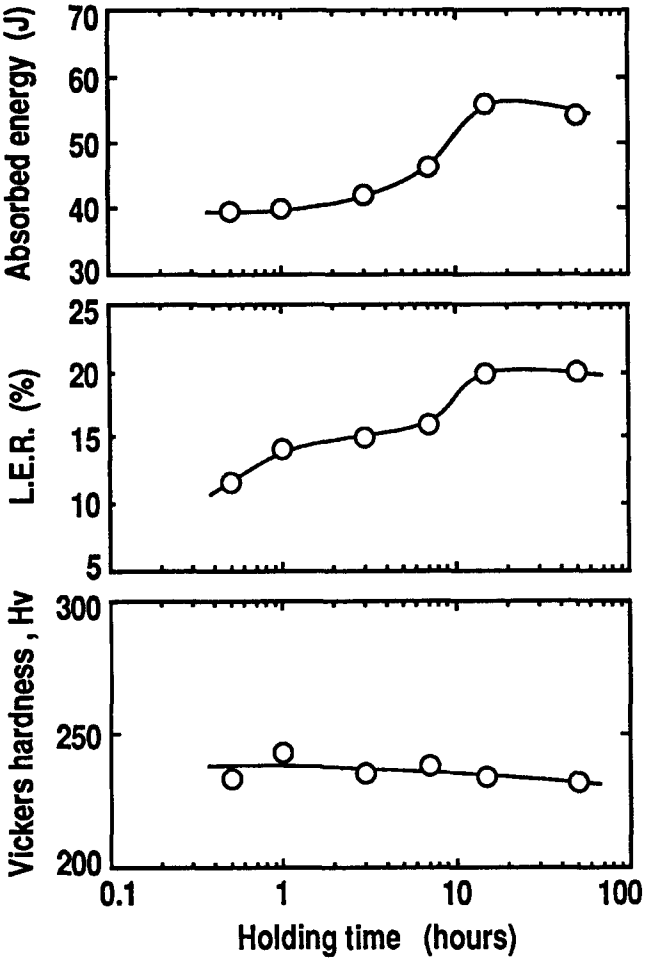

Fig. 2—Absorbed energy, lateral expansion ratio (LER), and Vickers hardness (Hv) as a function of holding time at the (α + γ) temperature range in QB' material.

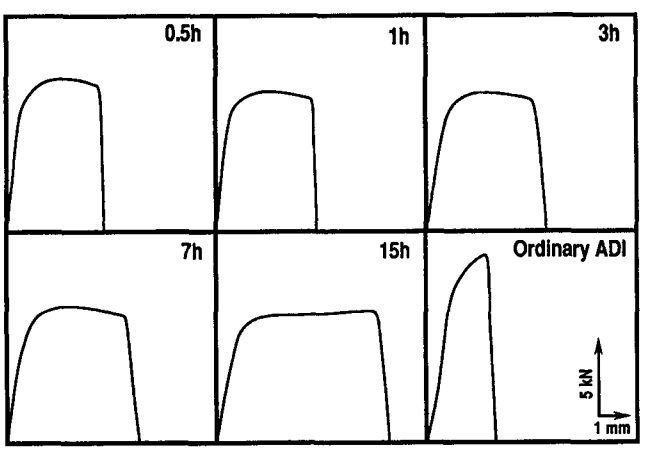

Fig. 3—Load *vs* load-point displacement curves obtained from the unnotched impact specimens of QB' materials with various holding times at the (α + γ) temperature range and ordinary ADI tested at room temperature.

C. *Scanning Electron Microscopy*

Samples for the scanning electron microscopy (SEM) observation of microstructures were prepared from the central region of the heat-treated Y-block sections and etched in 2 pct nital. Energy dispersive X-ray (EDX) analysis was performed to assess the concentration of alloying elements in ferrite, retained austenite, and carbide.

In order to observe the extent of void growth, the Charpy specimen fracture surfaces were examined by SEM.

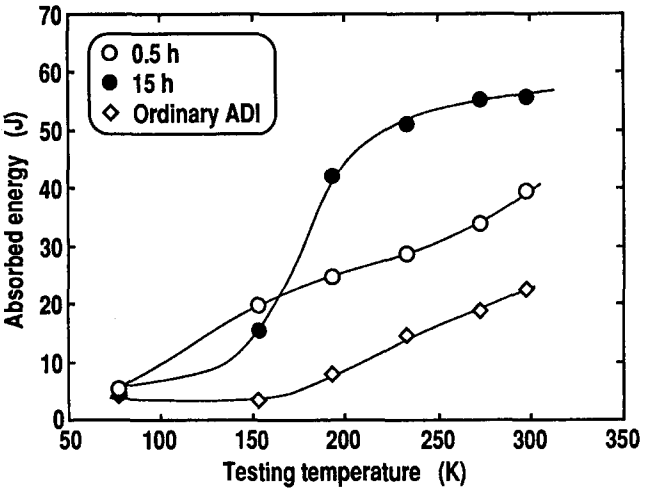

Fig. 4—Absorbed energy as a function of testing temperature in QB' materials with holding times of 0.5 and 15 h and ordinary ADI.

D. *Transmission Electron Microscopy*

Thin foil samples for the transmission electron microscopy (TEM) study were prepared using the atom beam etching method. The procedure consisted of the following steps: (1) the samples with a diameter of 3 mm and thickness of 1 mm were obtained from the heat-treated material by electrodischarge machining using a microcutting machine; (2) the samples were mechanically polished to approximately 50 μm using fine emery paper; and (3) atom beam etching was accomplished in argon. The thinning required approximately 30 hours at a 5 kV acceleration voltage and at an angle of 30 deg between the atom beam and the sample, followed by an additional 7 hours at a 4 kV acceleration voltage and at an angle of 15 deg.

Furthermore, in order to obtain the details of the precipitated carbide, the extraction replica method was used. The procedure for extraction replica consisted of the following steps: (1) carbides were extracted from the deeply etched samples using 0.08-mm-thick acetylcellulose film; (2) a carbon layer of approximately 20 nm in thickness was deposited onto the acetylcellulose film; and (3) the acetylcellulose film was decomposed by methyl acetate at approximately 50 °C, and the carbon film with the carbides was fixed on a copper microgrid.

III. EXPERIMENTAL RESULTS AND DISCUSSION

A. *Toughness Properties of QB' material*

Figure 2 shows the absorbed energy, lateral expansion ratio, and Vickers hardness of the QB' material as a function of holding time in the (α + γ) temperature range. The ab-

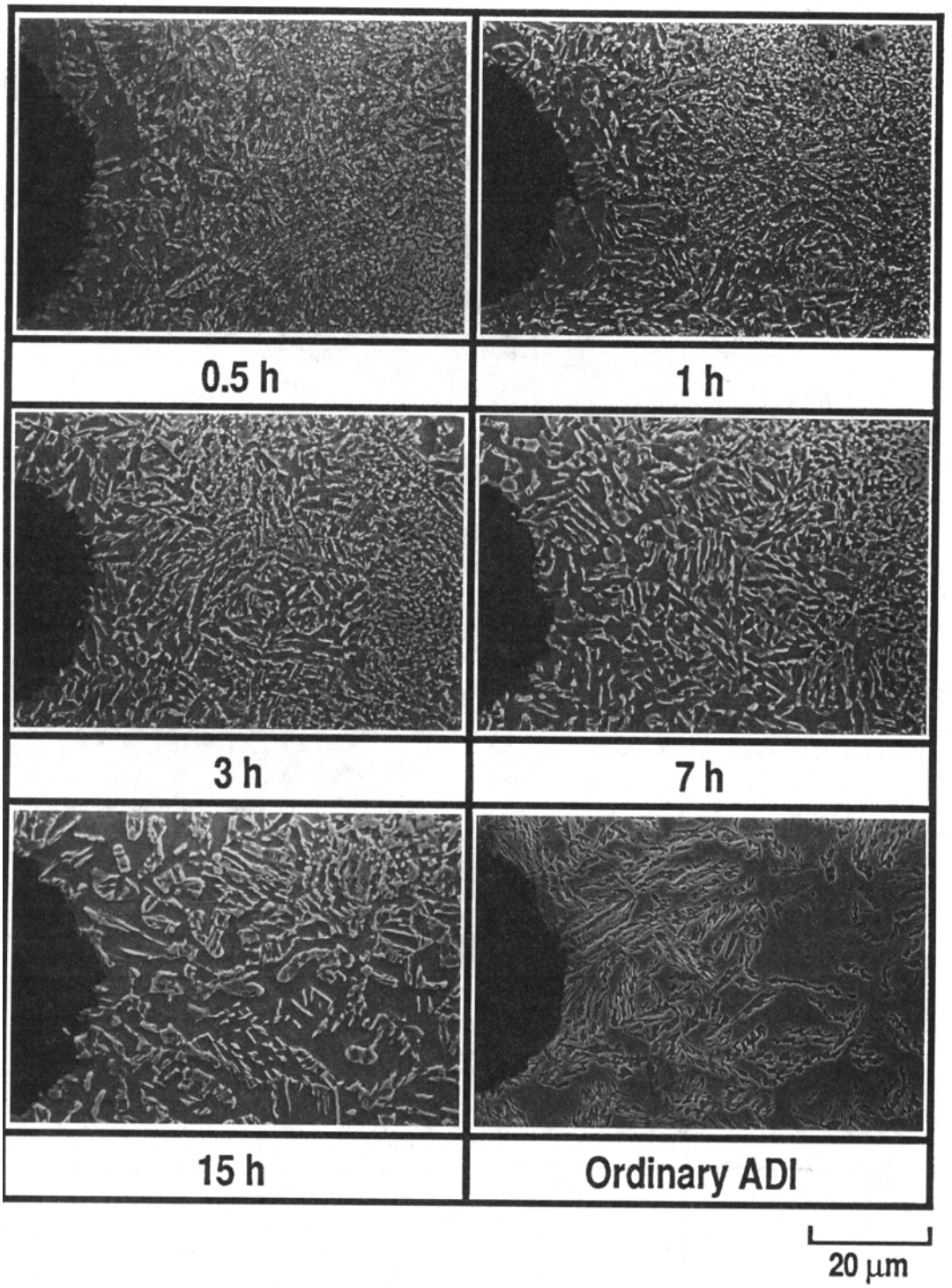

Fig. 5—Microstructure of QB' materials with various holding times at the (α + γ) temperature range and ordinary ADI (etched by 2 pct nital).

sorbed energy and the lateral expansion ratio increased with holding time, with no change after 15 hours. Vickers hardness showed little change over the holding time. Figure 3 shows the load-displacement curves obtained from the instrumented Charpy impact tests at room temperature. Here, it may be considered that the maximum load is nearly proportional to the static tensile strength. A 20 to 30 pct reduction in the strength level is observed as a function of holding time; *however*, the deflection to failure increased largely with increasing holding time. Thus, the increase in toughness is caused mainly by the increase in the ductility.

Figure 4 shows the ductile-brittle transition behavior of the QB' material (0.5 and 15 hours holding time) and ordinary ADI. The QB' material, held for 15 hours in the (α + γ) temperature range, surpassed the ordinary ADI 2.5 times in the upper-shelf energy. Furthermore, it showed bet-

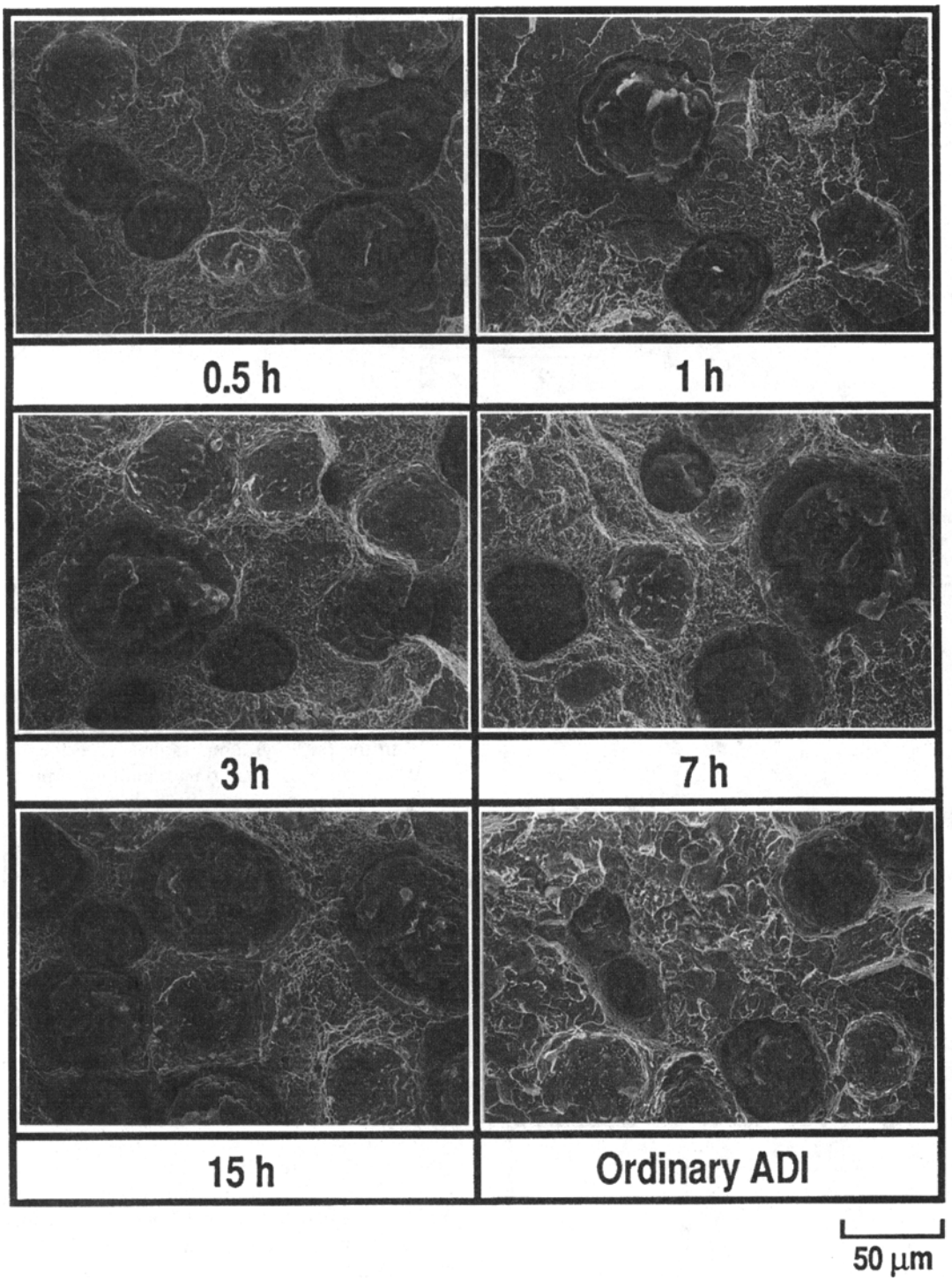

Fig. 6—SEM fractographs at the center of the fracture surface obtained from the un-notched impact specimens of QB' materials with various holding times at the (α + γ) temperature range and ordinary ADI tested at room temperature.

ter toughness compared with the QB' material held for 0.5 hours at test temperatures of −70 °C and above.

B. *Microstructure and Fracture Surface*

Microstructures and fracture surfaces were observed by SEM in order to understand the reason for the change in toughness, especially the ductility factor, as a function of holding time in the (α + γ) temperature range.

Figure 5 shows the microstructures of the QB' material and the ADI. The QB' material exhibited fine and uniform matrix without the γ pool. The latter was typically observed in the ordinary ADI. The retained austenite in the QB' material appears isolated by the ferrite phase, as the material

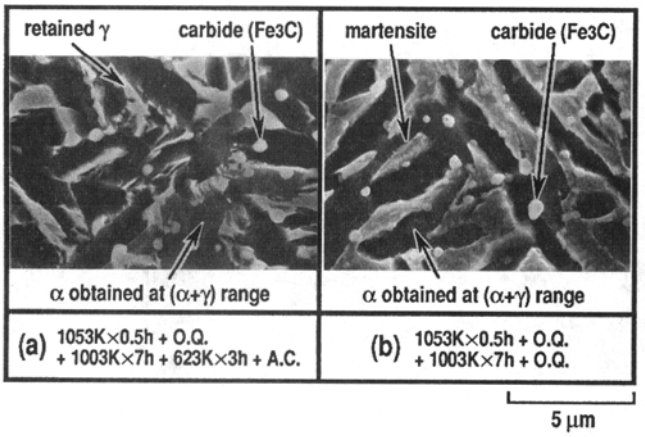

Fig. 7—(*a*) and (*b*) SEM micrographs of the specimen reaustenitized for 7 h.

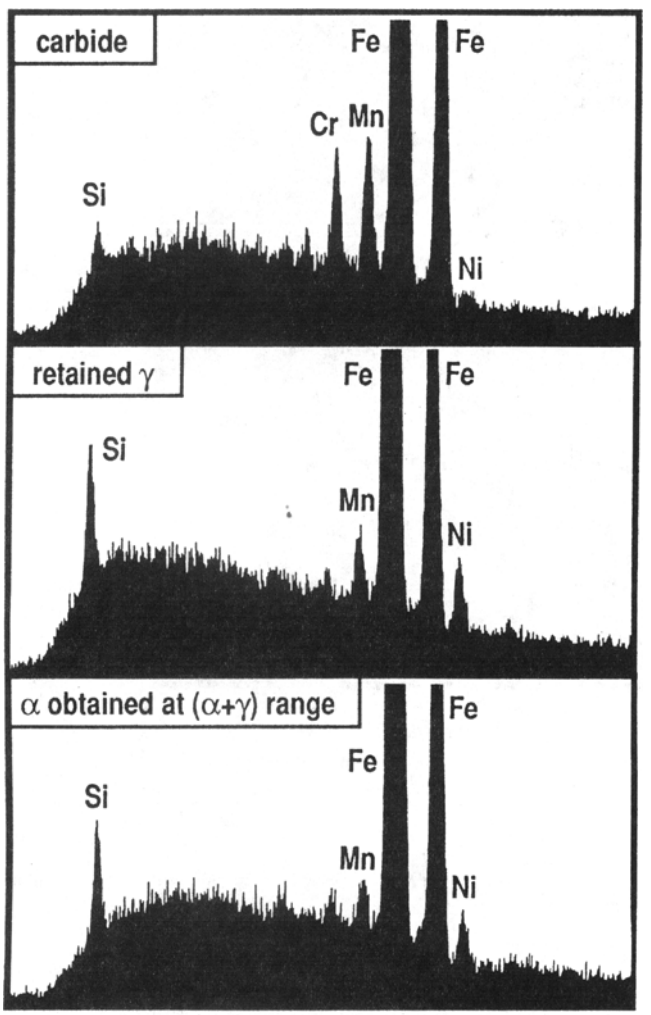

Fig. 8—EDX spectra of phases shown in Fig. 7(a).

was reaustenitized in the (α + γ) temperature range. Figure 6 shows the SEM fractographs at the center of specimens tested at room temperature. The void growth corresponding

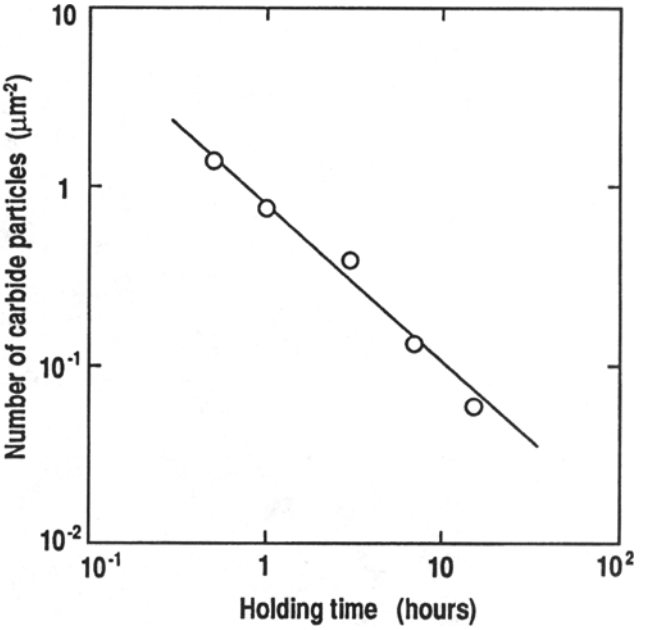

Fig. 9—Relationship between the number of carbide particles counted on SEM micrographs of etched materials and holding time at the (α + γ) temperature range.

to improved ductility can be observed in the QB' material held in the (α + γ) temperature range for a longer time.

While the QB' material exhibited improved toughness properties, the microstructure also revealed carbide particles, and the amount of carbide was found to decrease with increasing holding time in the (α + γ) temperature range. Generally, the carbide particles are known to act as sites for crack initiation. The formation and decomposition of the carbide particles, in the QB' process, are discussed in Section C.

C. *Formation Process of Carbides*

The carbide particles in the QB' material could be identified by SEM observation. Figure 7(a) shows the microstructure of the material held for 7 hours in the (α + γ) temperature range. Carbides were seen as fine particles in a matrix of ferrite and austenite. Carbide particles were also seen (Figure 7(b)) in the microstructure of the material immediately quenched after 7 hours of holding time without the isothermal treatment. This indicates that the carbide particles were already present in the material before the isothermal treatment.[10,11]

Figure 8 shows the results of EDX analysis for each phase shown in Figure 7(a). It was found that Mn and Cr, being carbide formation elements, were concentrated in the carbide. On the other hand, in the retained austenite phase, Mn and Ni, alloying elements known to stabilize the austenite phase, were slightly concentrated compared to the ferrite phase.

Figure 9 shows the number of carbide particles, estimated from the SEM micrographs, as a function of holding time in the (α + γ) temperature range. The following linear relationship on a logarithmic plot was obtained.

$$N = 0.803\ (t)^{-0.921} \qquad [1]$$

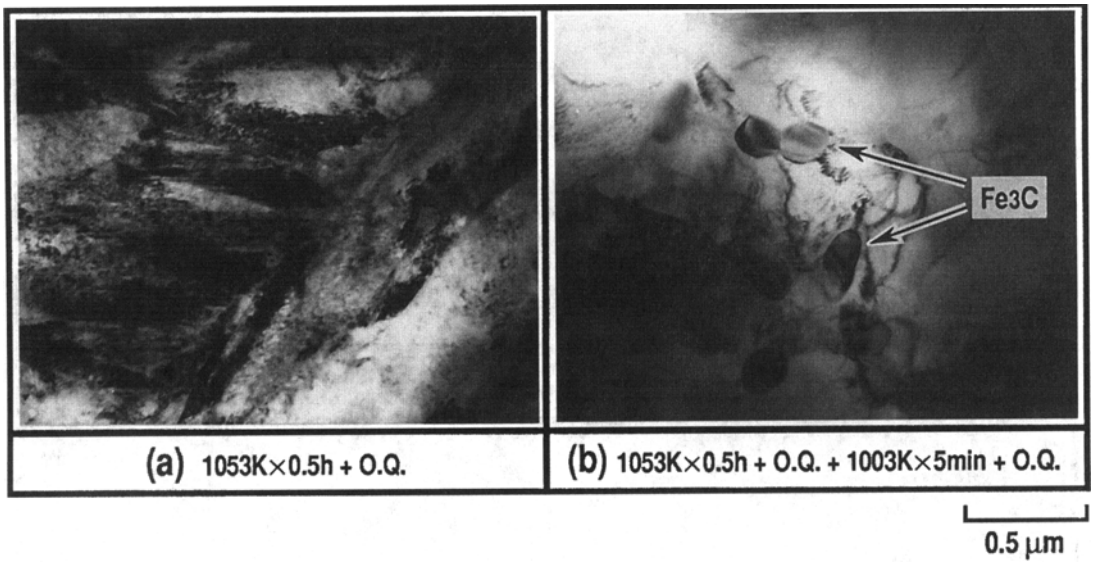

Fig. 10—(*a*) and (*b*) TEM micrographs of the thin foil obtained from as-quenched and quenched-tempered materials.

where N is the number of carbide particles (mm^{-2}) and t is the holding time (hours) in the ($\alpha + \gamma$) temperature range.

In order to further understand the formation process of the carbide, interrupted quench experiments were conducted and the prepared sections were examined by TEM. Figure 10(a) shows the TEM micrograph of the prequenched material before reaustenitization, and Figure 10(b) shows the TEM micrograph of the prequenched and reaustenitized material, with a 5-minute hold in the ($\alpha + \gamma$) temperature range followed by quenching. The prequenched material before reaustenitization showed martensitic structure without the carbide particles (Figure 10(a)), while in the reaustenitized material (Figure 10(b)), carbide particles were clearly seen. To assess the temperature at which the carbide precipitates, a series of quench experiments were performed at various temperatures during the reheating of the prequenched material. The TEM micrographs of extraction replicas, obtained from the materials heated to various temperatures up to the austenitizing temperature followed by quenching, are shown in Figure 11. A small amount of fine carbides was observed in the material heated to 300 °C, and the carbides of size 0.1 to 0.5 μm coexisted in the material heated up to 400 °C. It was found that these carbides have a structure of Fe_3C. At higher temperatures, only carbides of size 0.1 to 0.5 μm were observed.

The preceding study confirms that the carbide particles precipitate from the martensitic matrix during reaustenitization. The TEM micrographs of the QB' material with a 0.5-hour holding time in the ($\alpha + \gamma$) temperature range are shown in Figure 12. The micrographs in Figures 12(a) and (b) were obtained from thin films. Figure 12(c) shows the diffraction pattern corresponding to Figure 12(b). The micrograph in Figure 12(d) was produced from an extraction replica. It was found that the carbides have a structure of Fe_3C. One of the authors has reported that χ carbide was observed in the ADI material held for a long time at the austempering temperature.[10] However, no transition carbides were observed in this present study.

It is widely reported that secondary graphite is observed in quenched and tempered ductile iron, and the range of tempering temperature to form secondary graphite is 500 °C through 650 °C.[12,13,14] According to Voigt and Loper,[15] secondary graphite forms through the formation and decomposition of carbide, as well as directly by precipitation. They have also reported that the austenitizing temperature, at quenching, strongly influences the formation of secondary graphite, and an austenitizing temperature of approximately 930 °C gives the largest amount of secondary graphite. In the QB' process, the prequenched material is subjected to heating in the temperature range in which the secondary graphite is likely to precipitate. However, no secondary graphite was observed in the present work. This appears to be caused by the increase in the temperature for the decomposition of carbide due to the concentration of Mn and Cr as carbide formers (Figure 8). Furthermore, the formation of secondary graphite appears to be suppressed, as the austenitizing temperature at prequenching was low (780 °C) and the concentration of the alloying elements promoted carbide formation.

D. *Influence of Prior-Structure*

Prequenching in the QB' process is performed to enable precipitation of fine acicular ferrite during the austempering process. Moreover, the reason for the increase in toughness is the decomposition of carbide which forms in the martensitic prior-structure during the reheating process. Therefore, the precipitation of acicular ferrite and the effect of holding time on toughness are considered to change as a function of the prior-structure.

Figure 13 shows the microstructure and fracture surface in respect of FB' material (prior ferritic structure) held in the ($\alpha + \gamma$) temperature range for 0.5 and 15 hours. In the case of a ferritic prior-structure, austenite precipitation occurs in the prior ferrite grains and the holding time appears to cause coarsening of the microstructure. Fracture surfaces showed a mixture of dimple and cleavage morphologies in both materials with the holding time of 0.5 and 15 hours.

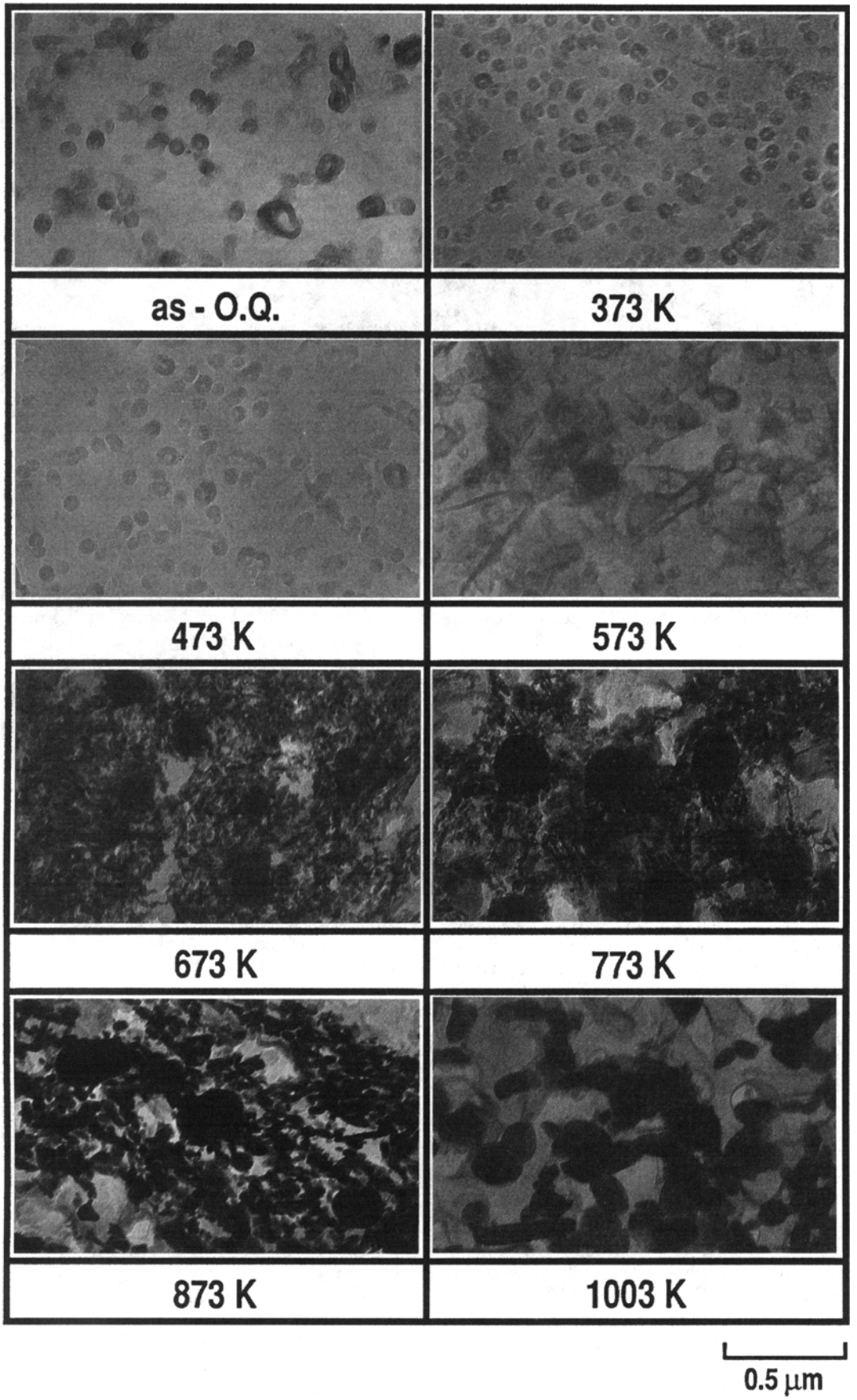

Fig. 11—TEM micrographs of the extraction replica obtained from material with various tempering temperatures. Both coarse and fine black particles are carbides.

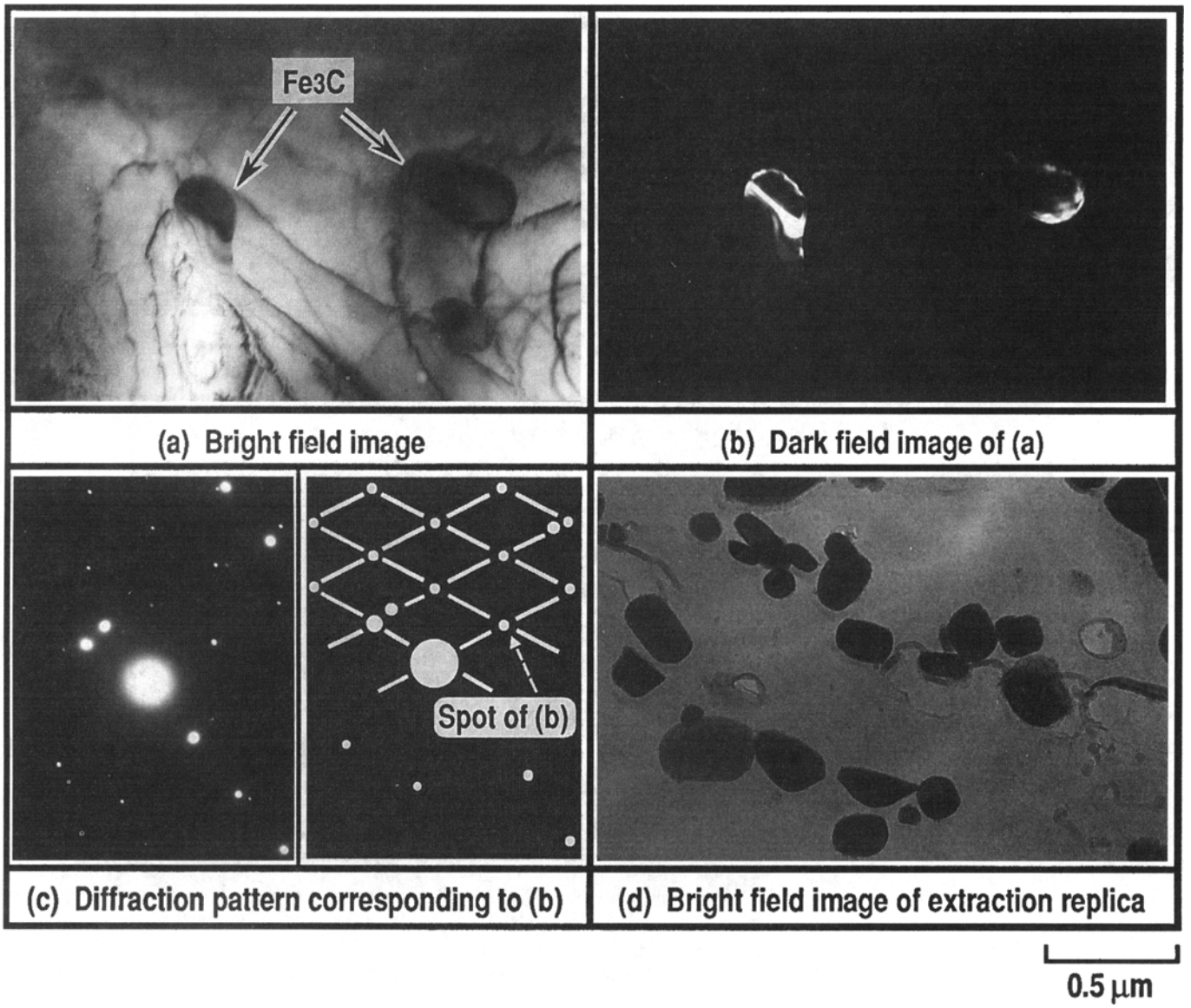

Fig. 12—(*a*) through (*d*) TEM micrographs of the thin foil and extraction replica obtained from the specimen reaustenitized for 0.5 h.

This suggests that the cleavage fracture easily occurs in the material with coarse ausferritic structures.

Figure 14 shows the microstructure and fracture surface for the PB' material which has a pearlitic prior-structure. Carbides were observed in the material even with the holding time of 15 hours. This indicates that a long holding time is necessary to decompose the relatively stable carbide around the eutectic cell boundary. Microvoids nucleated at carbides were observed in the matrix between the graphite nodules. Void growth observed on the fracture surface of the material with the holding time of 15 hours was larger than that with the holding time of 0.5 hours.

Figure 15 summarizes the effect of holding time in the (α + γ) temperature range on the toughness properties in ADI. Austempering from the (α + γ) temperature range (B' process) was effective for improving the toughness of ADI irrespective of the prior-structure. In the QB' and PB' processes, longer holding times resulted in the reduction of carbides, and the toughness increased with increasing holding time. Especially, the QB' material showed higher toughness compared with the others. Therefore, the refinement of matrix microstructure by prequenching is very effective in improving the toughness of ADI.

IV. CONCLUSIONS

A series of instrumented Charpy impact tests and the observation of the microstructure and fracture surface *via* SEM and TEM with EDX analysis were performed in order to examine the effect of holding time in the (α + γ) temperature range on toughness of specially austempered ductile iron. *Although some reduction (20 to 30 pct) in strength level occurred, twice or more improvement of the toughness could be expected in this treatment.*

1. In the case of the prequenched material, it was shown that the increase in toughness with the holding time in

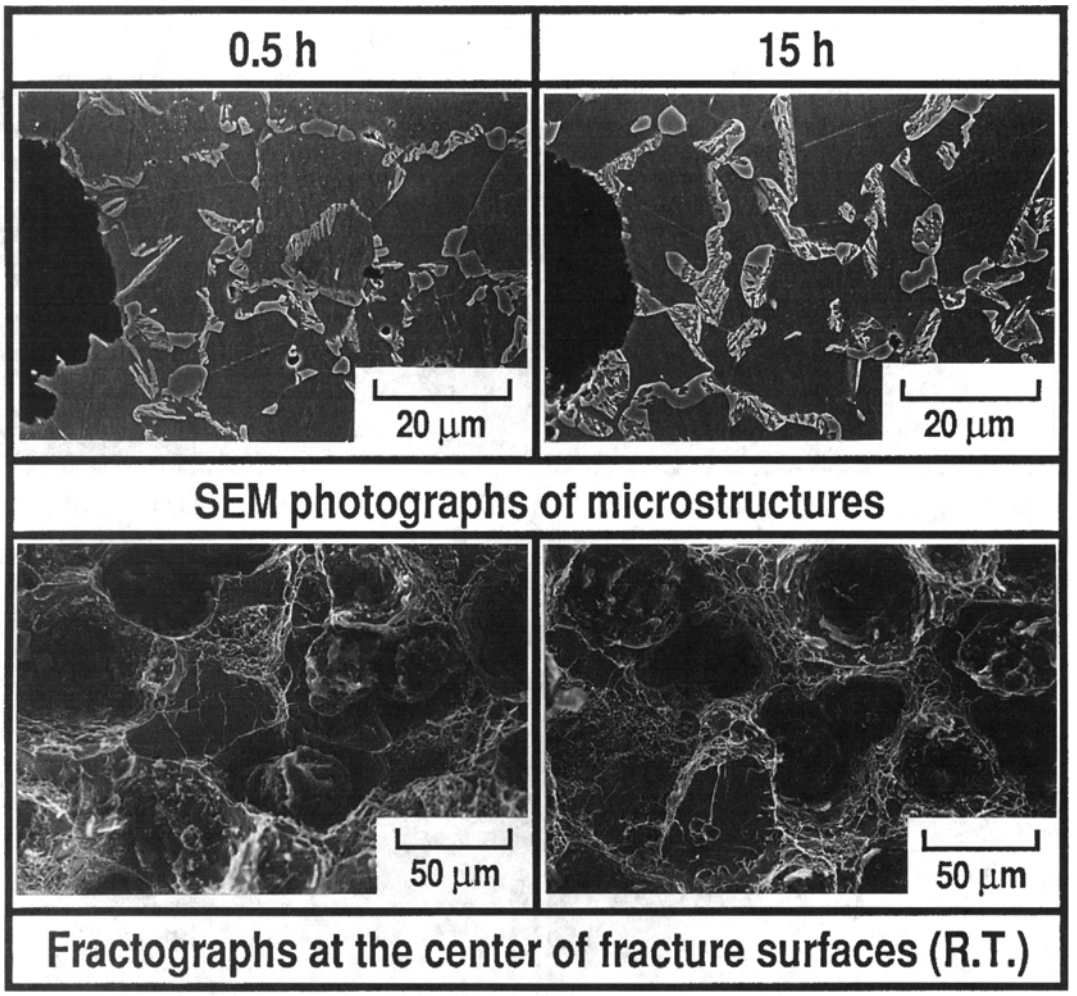

Fig. 13—Microstructures and fractographs of FB' materials reaustenitized for 0.5 and 15 h.

the (α + γ) temperature range was caused mainly by the increase in ductility due to the decomposition of carbide.
2. Carbides were seen to precipitate during the reheating process of the prequenched material, and their diameters in the final microstructure were 0.1 to 0.5 μm. These carbides were identified as $(Fe,Cr,Mn)_3C$. The reheating also resulted in the formation and decomposition of finer carbides.
3. In the case of a ferritic prior-structure, only marginal changes were observed in toughness with holding time in the (α + γ) temperature range, whereas in the case of a pearlitic prior-structure, toughness increased with increasing holding time, because the long heating time is necessary to decompose the relatively stable carbide around the eutectic cell boundary.

ACKNOWLEDGMENTS

The authors wish to thank Professor M. Niinomi and Dr. S. Seetharamu, Toyohashi University of Technology, Toyohashi, Japan, for their critical reading of the manuscript. They also extend their thanks to M/S Kurimoto, Ltd., for supplying the material. The authors also thank the reviewers for the constructive suggestions.

REFERENCES

1. O. Yanagisawa, T. Yano, and H. Fukuhara: *J. Jpn. Soc. Heat Treat. (Netsushori)*, 1988, vol. 28, pp. 314-19.
2. T. Yoshida, K. Komatsu, and S. Okada: *Hitachi Met. Tech. Rev.*, 1992, vol. 8, pp. 73-78.
3. T. Kobayashi and H. Yamamoto: *Metall. Trans. A*, 1988, vol. 19A, pp. 319-27.
4. T. Kobayashi and H. Yamamoto: *Trans. Jpn. Foundrymen's Soc.*, 1989, vol. 8, pp. 30-34.
5. S. Yamada, T. Kobayashi, and K. Matsuo: *8th Int. Congr. on Heat Treatment of Materials*, Kyoto 1992, Heat & Surface '92, Jap. Technical Inform. Serv., Tokyo, pp. 203-06.
6. T. Kobayashi, F. Kawakubo, and H. Yamamoto: *J. Jpn. Foundrymen's Soc. (Imono)*, 1986, vol. 58, pp. 130-35.
7. M. Aoyama, T. Kobayashi, and K. Matsuo: *Trans. Jpn. Foundrymen's Soc.*, 1993, vol. 12, pp. 52-61.
8. T. Kobayashi, I. Yamamoto, and M. Niinomi: *J. Test. Eval.*, 1993, vol. 21, pp. 145-53.
9. I. Yamamoto and T. Kobayashi: *Int. J. Pres. Ves. Piping*, 1993, vol. 55, pp. 295-312.

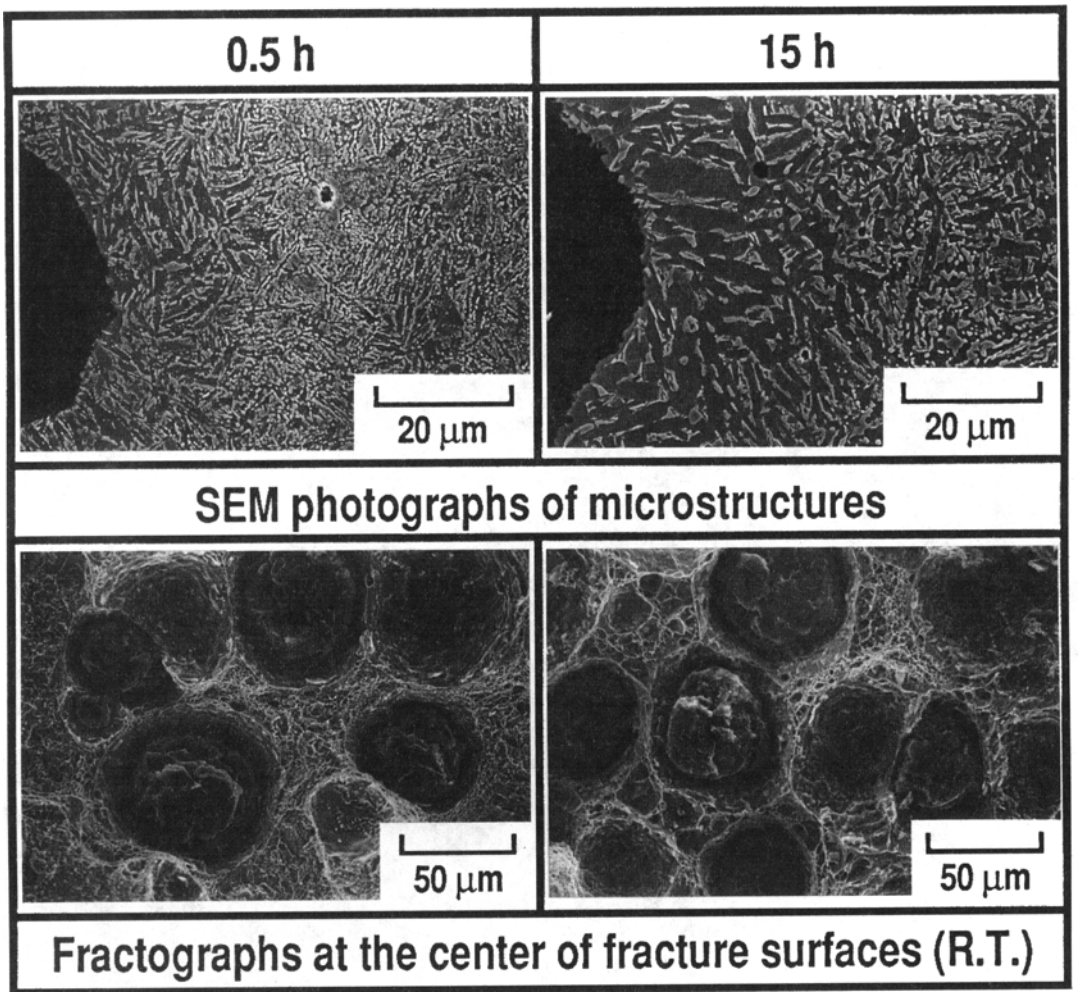

Fig. 14—Microstructures and fractographs of PB' materials reaustenitized for 0.5 and 15 h.

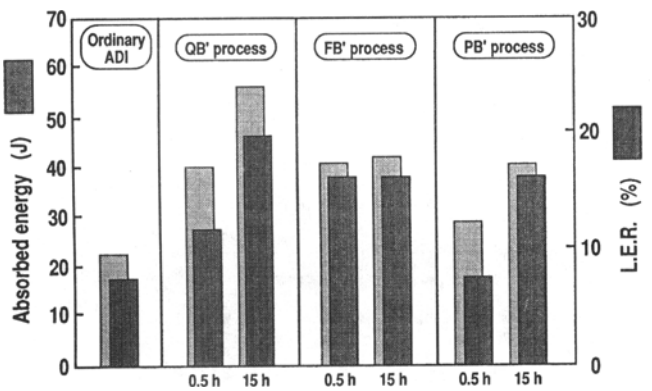

Fig. 15—Absorbed energy and LER in various heat-treated materials.

10. H. Yamamoto and T. Kobayashi: *Proc. 4th Int. Conf. Physical Metallurgy of Cast Iron*, Tokyo, Sept. 1990, Materials Research Society, Pittsburgh, PA, 1990, pp. 243-50.
11. W.J. Dubensky and K.B. Rundman. *AFS Trans.*, 1985, vol. 98, pp. 389-94.
12. G.A. Sandoz, H.F. Bishop, and W.S. Pellini: *Trans. ASM*, 1956, vol. 48, pp. 971-85.
13. A.K. Chakrabarti and P.P. Das: *Br. Foundryman*, 1975, vol. 68, pp. 1-8.
14. R.N. Vaid and V. Seshadri: *Trans. Ind. Inst. Met.*, 1969, vol. 22, pp. 22-26.
15. R.C. Voigt and C.R. Loper, Jr.: *AFS Trans.*, 1982, vol. 95, pp. 239-55.